Research Paper
Computational Methods for Differential Equations
http://cmde.tabrizu.ac.ir
Vol. *, No. *, *, pp. 1-21
DOI:10.22034/cmde.2026.69000.3384

Development and error analysis of a Novel FEM for convection–diffusion–reaction equations

Sadia Akter Lima[1], Md. Shafiqul Islam[2], Runchang Lin[3], and Md. Kamrujjaman[4,*]
[1]Department of Applied Mathematics, Noakhali Science and Technology University, Noakhali 3814, Bangladesh.
[2]Department of Applied Mathematics, University of Dhaka, Dhaka 1000, Bangladesh.
[3]Department of Mathematics and Physics, Texas A&M International University, TX 78041, USA.
[4]Department of Mathematics, University of Dhaka, Dhaka 1000, Bangladesh.

Abstract

This study examines the Finite Element Method (FEM) as an effective numerical approach for solving two-dimensional (2D) higher-order, non-homogeneous, and nonlinear convection–diffusion–reaction (CDR) equations. A key focus is on the convergence and stability analysis of nonlinear parabolic partial differential equations (PDEs) and the CDR model. Unlike conventional methods that simplify nonlinearity through assumptions, our approach retains the full complexity of the equations, demonstrating the robustness and versatility of FEM. We apply FEM to unsteady-state problems, emphasizing its accuracy and computational efficiency. Various error analyses validate the reliability of the method. To further assess its performance, we conduct extensive numerical experiments, with graphical representations reinforcing the accuracy and stability of FEM in solving spatially distributed 2D CDR equations. The results establish FEM as a powerful and reliable tool for solving nonlinear PDEs while maintaining computational stability and practical applicability. Its ability to handle intricate nonlinear dynamics without restrictive assumptions highlights its potential in real-world applications. The study affirms that FEM is not only efficient but also a versatile numerical technique for solving complex 2D parabolic PDEs and CDR models, making it a valuable asset in scientific and engineering computations.

Keywords. Nonlinear PDE, Finite element method, CDR equation, Error analysis.
2010 Mathematics Subject Classification. 92D25, 35K57 (primary), 35K61, 37N25.

1. Introduction

A wide variety of parabolic PDEs arise in applications and are effective in describing the evolution of processes that depend on independent variables, such as population spread, heat transfer, and fluid flow [29, 31]. Consider the CDR equation over the spatial domain $(x, y) \in \Omega \subset \mathbb{R}^2$, defined as:

$$\partial_t U(x,y,t) + U(x,y,t)\nabla U(x,y,t) = C\,\nabla^2 U(x,y,t) + f(U(x,y,t)).$$

Without the convection term $U(x,y,t)\nabla U(x,y,t)$, the CDR equation is referred to as the Kolmogorov–Petrovsky–Piskunov equation. The equation represents a diffusion–reaction process when the convection term vanishes. In this equation, $U = U(x,y,t)$ acts as a state variable, where $(x,y) \in \Omega \subset \mathbb{R}^2$. After that, $C\,\nabla^2 U(x,y,t)$ acts as the diffusion term, where C is the diffusion coefficient. The last term $f(U(x,y,t))$ appears as a smooth function and explains the actual process of modification of U.

To overcome these challenges, scientists and researchers have been developing suitable techniques and seeking corresponding analytical solutions. In the field of numerical analysis of differential equations, various methods are employed, including the FDM [40], Galerkin and modified Galerkin methods [13, 22, 23], the shooting method [10], the sub-domain least squares method [36], and the decomposition method [43]. However, these methods may not be suitable for obtaining numerical solutions at specific grid points, and the computational cost required to achieve

Received: 05 September 2025; Accepted: 09 August 2026.
* Corresponding author. Email: kamrujjaman@du.ac.bd.

higher accuracy can be quite prohibitive. These drawbacks can be overcome by applying the FEM, which is capable of providing approximate solutions in complex domains. Because of its significant potential, the widely applied FEM has drawn the attention of many researchers. In various important applications within the field of medical science, mathematical models play an essential role in formulating two-dimensional parabolic PDEs. These equations often involve nonlocal boundary conditions as well as Dirichlet boundary conditions, and they have been studied extensively in the literature. The FEM was applied in [30, 40] to obtain approximate solutions of PDEs. Capasso and Kunisch [12] studied a reaction–diffusion system representing a model of man–environment diseases. Some researchers have also been interested in developing numerical schemes for diffusion equations, as reported in [41]. Cannon *et al.* were able to obtain approximate solutions of a diffusion equation in two spatial variables [11], and this equation with a nonlocal boundary condition was studied in [35] by employing the explicit FEM. Mohammad solved a similar equation with an integral condition using the Crank–Nicolson scheme [28].

In this study, we focus on applying FEM to evaluate the solutions of two-dimensional spatial CDR problems. In [34], Neville *et al.* considered the FEM for time-fractional PDEs. Jiang and Ma [21] established a higher-order method based on FEM and FDM for space and time discretizations, respectively. George *et al.* made a comparison between FEM and FDM for 2D elliptic PDEs [19]. Chen and Li conducted a study on time-fractional PDEs with damping and introduced an Alternating Direction Implicit (ADI) Galerkin method [14]. They demonstrated the unconditional stability and convergence of the method and performed a comparative analysis between numerical and theoretical results.

Importantly, time-fractional partial integro-differential equations were analyzed in [17] for some specific nonlinear problems. The authors used the weighted and shifted Grünwald–Letnikov formula to approximate the Caputo fractional derivative, and the fractional trapezoidal rule was applied to the Volterra integral operator. Chebyshev nodes and the spectral collocation method were implemented for spatial discretization, while the finite block method was incorporated to handle irregular computational domains in two-dimensional cases. The nonlinear problem was transformed into a linear form using quasilinearization. Additionally, they analyzed their proposed technique in terms of stability and convergence and confirmed its accuracy and efficiency through numerical experiments. Another study [16] solved nonlinear distributed-order space–time fractional PDEs in one and higher dimensions using an efficient numerical method, which combines the finite element approach for spatial discretization with the second-order backward differentiation formula, composite trapezoidal rule, and weighted shifted Grünwald–Letnikov approximation for time discretization. The stability and convergence of the proposed method were analyzed in the study, and the accuracy and reliability of the method were confirmed through numerical results. Moreover, the weighted and shifted Grünwald–Letnikov formula with BDF2 was introduced in [1]. The fractional trapezoidal rule, Chebyshev nodes with collocation, and the finite block method were applied for time, space, and irregular domains, respectively, while quasilinearization was used to handle nonlinearity. Finally, the stability and convergence of the proposed approach were investigated, and its accuracy was confirmed through numerical experiments. Another related study [18] considered a distributed-order time-fractional partial integro-differential equation in one and higher dimensions and used a graded time mesh. Chebyshev collocation and a hybrid ADI approach were applied for spatial discretization, while the integral terms and time-fractional derivative were approximated numerically. Irregular domains were handled by the finite block method. Numerical results confirmed the accuracy and efficiency of the proposed method after analyzing its stability and convergence.

Ali and Kamrujjaman applied the Generalized Finite Element Method (GFEM) in [6] to solve nonlinear parabolic PDEs featuring Robin boundary conditions. They also ensured the stability of their numerical scheme and performed a comparative study between analytical and numerical results to establish the efficiency and reliability of the GFEM [15]. In [5], Ali and his colleagues presented a numerical technique derived from GFEM for obtaining highly accurate numerical solutions of reaction–diffusion equations. These equations include Burgers' equation, Fisher's equation, the Newell–Whitehead–Segel equation, and the Burgers–Huxley equation. Convergence and stability analyses of the method have been illustrated in this paper.

Notably, four iterative methods, namely, Broyden's Method (BM), Optimal Fourth-Order Method (OFOM), Optimal Sixth-Order Method (OSOM), and the Homotopy Continuation Method (HCM), were analyzed to determine which one is more applicable for solving real-world nonlinear models in [4, 9, 42]. With the fractional-order Bagley–Torvik equation finding various applications in daily life, a novel numerical scheme was introduced in [3, 38]. This scheme has been demonstrated to offer sustained accuracy. Ali and his colleagues also verified the effectiveness of the GFEM by solving the prominent FitzHugh–Nagumo equation in [2].

Furthermore, Lima and others outlined the formulation and solution procedure of a robust FEM in [24, 25] for obtaining numerical solutions of CDR equations and parabolic PDEs. In [24], they tackled the FitzHugh–Nagumo equation and Fisher's equation with stable and unstable geometrical shapes, comparing numerical solutions with exact solutions to demonstrate the capabilities and potential of FEM. Moreover, the paper [25] presented an analysis of convergence and stability for nonlinear parabolic PDEs. Finally, this research work assessed dissipation error, dispersion error, and total error to verify the accuracy of the introduced method.

Considering these research papers, we are inspired to work with PDEs by applying FEM over a two-dimensional spatial domain. The 2D CDR equation is an important model because of its enormous applications in the fields of science, finance, biology, epidemiology, engineering, and real life. Sequentially, we require accurate numerical solutions of the 2D CDR model, which has motivated us to complete this work. The FEM is a significant numerical technique for finding solutions to problems with general geometry. In this paper, we address the 2D CDR problem using FEM while imposing Dirichlet boundary conditions:

$$
\begin{cases}
\mu(x,y)\,U_t(x,y,t) + U(x,y,t)\nabla U(x,y,t) = \alpha_1(x,y)\,U_{xx}(x,y,t) + \alpha_2(x,y)\,U_{yy}(x,y,t) \\
\qquad\qquad\qquad\qquad\qquad\qquad\qquad -\beta(x,y)\,U(x,y,t) + f(U(x,y,t)), \\
t \in (0,T],\ (x,y) \in \Omega \equiv [p,q] \times [r,s], \\
U(x,y,0) = U_0(x,y),\ (x,y) \in \Omega, \\
U(p,y,t) = U_p(y,t), \quad U(q,y,t) = U_q(y,t), \quad t > 0,\ y \in [r,s], \\
U(x,r,t) = U_r(x,t), \quad U(x,s,t) = U_s(x,t), \quad t > 0,\ x \in [p,q].
\end{cases}
\tag{1.1}
$$

In the two-dimensional system described in Equation (1.1), the function $U(x,y,t)$ represents various factors such as heat and diffusion, and $U(x,y,t)\nabla U(x,y,t)$ is the nonlinear convection term. The term $\alpha_1(x,y)\,U_{xx}(x,y,t) + \alpha_2(x,y)\,U_{yy}(x,y,t)$ represents diffusion, where the parameters α_1 and α_2 correspond to diffusion coefficients in the system, and the reaction term is $f(U(x,y,t))$. Here, $U_p(y,t)$, $U_q(y,t)$, $U_r(x,t)$, and $U_s(x,t)$ are functions of the spatial variables $(x,y) \in \Omega$ and time t. The initial condition, U_0, represents the initial density, which may be constant or a function of the spatial variables (x,y). The spatial variable x ranges from the initial boundary point p to the terminal point q, while the variable y ranges from the initial boundary point r to the terminal boundary point s. It is assumed that the reaction term $f(U(x,y,t))$ exhibits a satisfactory level of smoothness. To simplify our work throughout the paper, we introduce the notation $\mathcal{D} = \Omega \times (0,T]$, with $T > 0$, and $\Omega \equiv [p,q] \times [r,s]$, such that $(x,y,t) \in \mathcal{D}$.

The innovative aspect of this study is the incorporation of a simple and efficient linear FEM for finding solutions to two-dimensional nonlinear CDR equations while maintaining the full nonlinear behavior of the model. Our proposed method is capable of maintaining accuracy with remarkably reduced CPU time and simpler implementation, while higher-order finite elements or FDM provide similar accuracy with higher computational cost due to complex calculations. A comprehensive stability and convergence analysis is performed, along with a detailed assessment of quantification errors to ensure the accuracy and acceptability of the introduced technique. A comparative study with FDM and quadratic FEM confirms that all approaches produce nearly identical approximations, while our proposed approach remains computationally more efficient and easier to implement. Furthermore, approximate solutions using linear FEM are evaluated and compared for different values of the total time T, corresponding to different numbers of elements, to investigate the behavior of the proposed method. Three numerical experiments are included to confirm the effectiveness and reliability of the method, and to highlight its potential, robustness, and applicability to non–linear parabolic PDEs and CDR models.

The proposed work is organized as follows:

In Section 2, we explore the implementation of a weak formulation of FEM for the 2D general CDR model (1.1). This model serves as the cornerstone equation in this paper. Moving forward to Section 3, our focus shifts to the convergence and stability analysis of FEM as applied to the 2D governing CDR system (1.1). This section aims to ensure the effectiveness and precision of the method. To further ascertain the efficacy and accuracy of our approach, Section 4 is dedicated to the presentation of quantification error analysis. In Section 5, the weak formulation is put into practice through the numerical analysis of 2D boundary value problems. Then, tabulated approximate data are provided. Furthermore, an extensive exploration of various error types forms an integral part of our work, and this analysis is incorporated within the same section. Additionally, a comparison table is included to compare the results of the proposed technique with two existing methods, quadratic FEM and FDM. Finally, a new table is added to compare CPU time and maximum error of these three methods. Within this section, efforts are made to visually compare theoretical predictions and numerical outcomes for different time steps. Importantly, this section also contains a comparative study at total time $T = 10$ for three different time steps to understand its limiting behavior. Lastly, we reach the culmination of our study in Section 6, where we draw conclusions, offer remarks, and provide a broader discussion to give a comprehensive wrap-up of the paper.

In the subsequent Section 2, we now proceed to apply the weak formulation of the FEM to the nonlinear CDR equation in a two-dimensional context.

2. Weak Formulation of the FEM for the CDR Equation

In this section, we derive the weak formulation of FEM for the CDR equations, which describes diffusion processes in two-dimensional space. Here, “convection” signifies the movement-related transport occurring within a fluid or gas. It involves the rising of hotter, less dense materials and the sinking of colder, denser materials.“Reaction” refers to interactions within the system, and “diffusion” denotes the uniform distribution of components through movement from areas of higher concentration to those of lower concentration, and vice versa. Concisely, a mathematical CDR model represents the distribution of the concentration of the components. For applying FEM to solve CDR equations, it is necessary to understand elements, as they are used to discretize complex geometries into simpler, interconnected shapes. A segment of the problem domain is called an element, $[e]$. It may take various simple shapes such as a straight line in 1D, a triangle or quadrilateral in 2D, or a tetrahedron or rectangular solid in 3D.

To establish the weak formulation of Eq. (1.1), we consider the trial solution as follows:

$$\tilde{U}(x,y,t) = \sum_{j=1}^{n} a_j(t)\psi_j(x)\psi_j(y), \tag{2.1}$$

where a_j is a function of t.

Consequently, we obtain the following derivatives

$$\tilde{U}_t = \sum_{j=1}^{n} \frac{da_j(t)}{dt}\psi_j(x)\psi_j(y),\ \tilde{U}_x = \sum_{j=1}^{n} \frac{d\psi_j(x)}{dx}a_j(t)\psi_j(y),\ \tilde{U}_y = \sum_{j=1}^{n} \frac{d\psi_j(y)}{dy}a_j(t)\psi_j(x).$$

The weighted residual equation of the CDR model in two-dimensional space for a particular element $[e]$ is:

$$\begin{aligned}
&\iint_e \Big[\mu\,\tilde{U}_t + \tilde{U}\,\nabla\tilde{U} - \alpha_1\tilde{U}_{xx} - \alpha_2\tilde{U}_{yy} + \beta\tilde{U}(x,y,t) - f(\tilde{U}(x,y,t))\Big]\psi_i(x)\psi_j(y)\,dxdy = 0,\\
&\Rightarrow \iint_e \mu\tilde{U}_t\psi_i(x)\psi_i(y)dxdy + \iint_e \tilde{U}\,\nabla\tilde{U}\psi_i(x)\psi_i(y)dxdy - \iint_e \alpha_1\tilde{U}_{xx}\psi_i(x)\psi_i(y)dxdy\\
&- \iint_e \alpha_2\tilde{U}_{yy}\psi_i(x)\psi_i(y)dxdy + \iint_e \beta\tilde{U}(x,y,t)\psi_i(x)\psi_i(y)dxdy - \iint_e f(\tilde{U}(x,y,t))\psi_i(x)\psi_i(y)dxdy = 0,\\
&\Rightarrow \mu\iint_e \sum_{j=1}^{n}\frac{da_j(t)}{dt}\psi_j(x)\psi_j(y)\psi_i(x)\psi_i(y)dxdy + \iint_e \sum_{j=1}^{n}\nabla\tilde{U}a_j(t)\psi_j(x)\psi_j(y)\psi_i(x)\psi_i(y)dxdy\\
&- \int_e \left[\alpha_1\left[\tilde{U}_x\psi_i(x)\right]_e - \alpha_1\int_e\left[\frac{d\psi_i}{dx}\sum_{j=1}^{n}\frac{d\psi_j(x)}{dx}a_j(t)\psi_j(y)\right]dx\right]\psi_i(y)dy
\end{aligned}$$

$$-\int_e \left[\alpha_2 \left[\tilde{U}_y \psi_i(y)\right]_e - \alpha_2 \int_e \left[\frac{d\psi_i}{dy}\sum_{j=1}^{n}\frac{d\psi_j(y)}{dy}a_j(t)\psi_j(x)\right] dy\right] \psi_i(x)dx$$
$$+ \iint_e \beta \sum_{j=1}^{n} a_j(t)\psi_j(x)\psi_j(y)\psi_i(x)\psi_i(y)dxdy - \iint_e f(\tilde{U}(x,y,t))\psi_i(x)\psi_i(y)dxdy = 0. \tag{2.2}$$

To achieve greater precision in the results and to streamline the computational process, we may consider using linear basis functions instead of quadratic ones for triangular, rectangular, and other element types. Thus, the recommended basis functions are:

$$P_1(\Psi) = \frac{(1-\Psi)}{2},\ P_2(\Psi) = \frac{(1+\Psi)}{2},\ \Psi \in [-1,1]. \tag{2.3}$$

Now, for convenience, we finalize the simplification process and obtain the standard matrix form as follows:

$$\frac{da_j(t)}{dt}C_{i,j} + K_{i,j}a_j(t) = F_i(t), \tag{2.4}$$

$$\begin{cases} K_{i,j} = A_{i,j} + B_{i,j} + M_{i,j} + N_{i,j}, \quad C_{i,j} = \mu \sum_{j=1}^{n} \iint_e \psi_i(x)\psi_j(x)\psi_i(y)\psi_j(y)dxdy, \\ A_{i,j} = \iint_e \alpha_1 \left[\frac{d\psi_i}{dx}\sum_{j=1}^{n}\frac{d\psi_j(x)}{dx}\psi_j(y)\right]\psi_i(y)dxdy, \quad B_{i,j} = \iint_e \alpha_2 \left[\frac{d\psi_i}{dy}\sum_{j=1}^{n}\frac{d\psi_j(y)}{dy}\psi_j(x)\right]\psi_i(x)dxdy, \\ M_{i,j} = \iint_e \sum_{j=1}^{n} \nabla\tilde{U} a_j(t)\psi_j(x)\psi_j(y)\psi_i(x)\psi_i(y)dxdy, \quad N_{i,j} = \iint_e \beta \sum_{j=1}^{n}\psi_j(x)\psi_j(y)\psi_i(x)\psi_i(y)dxdy, \\ F_i(t) = \iint_e f(\tilde{U}(x,y,t))\psi_i(x)\psi_i(y)dxdy + \int_e \alpha_1[\tilde{U}_x\psi_i(x)]_e\psi_i(y)dy + \int_e \alpha_2[\tilde{U}_y\psi_i(y)]_e\psi_i(x)dx. \end{cases}$$

Frequently, $C_{i,j}$ is referred to as the capacity or heat capacity integral, and $C = [C_{i,j}]$ is known as the capacity matrix. In this context, it is convenient to consider a finite number of elements obtained by partitioning the whole domain and to evaluate the above matrices for each element using the chosen basis functions. After assembly, the following compatible matrix form (2.5) can be obtained as:

$$C\dot{U} + KU = F. \tag{2.5}$$

In summary, Eq. (2.5) represents a system of first-order differential equations with a single independent variable t, and $\dot{U}$ can be discretized as follows:

$$\dot{U} = \frac{U_{j+1} - U_j}{\Delta t}. \tag{2.6}$$

Here, it is required to use a particular value of Δt. Afterwards, applying Eq. (2.6), Eq. (2.5) can be rearranged as:

$$CU_{j+1} + (K\Delta t - C)U_j = F\Delta t. \tag{2.7}$$

At this stage, U_{j+1} represents the nodal values, which can be obtained by applying a suitable method along with appropriate initial conditions.

In Section 3, we analyze the convergence and stability of the model.

3. Analysis of convergence and stability

Let $P_i(\Psi) \in \mathbb{H}_2^1(\Omega)$, $i = 1, 2, 3, \ldots, n$, where $P_i(\Psi)$ denotes the space of basis functions and $\mathbb{H}_2^1(\Omega) \equiv W^{1,2}(\Omega)$ is a Sobolev (Hilbert) space with $p = 2$. The space is equipped with the norm

$$\|v\|_{\mathbb{H}_2^1(\Omega)} = \left(\int_\Omega v^2\,dx + \int_\Omega |\nabla v|^2\,dx\right)^{1/2}.$$

This space is complete and plays a fundamental role in weak formulations of PDEs.

In Eq. (1.1), the constants α_i, $i = 1, 2$, are known as the coefficients of the diffusion term, and $\beta(x, y)U(x, y, t)$ and $f(U(x, y, t))$ are continuous functions. Therefore, Eq. (1.1) admits a unique solution [33]. The compatible matrix form (2.4) can be rewritten as (3.1) by substituting the trial solution (2.1) into (1.1) as follows:

$$\frac{dU}{dt} + C^{-1}KU = C^{-1}F. \tag{3.1}$$

Eq. (3.1) can be written as an initial value problem as follows:

$$\begin{aligned} &\frac{dU_i}{dt} + (\Phi_i + \Phi_j)\, U_i = \tau_i\, \tau_j, \\ &U_i(0) = \psi(\eta). \end{aligned} \tag{3.2}$$

At this stage, the integrating factor for Eq. (3.2) is:

$$e^{\int(\Phi_i+\Phi_j)dt} = e^{(\Phi_i+\Phi_j)t}. \tag{3.3}$$

To evaluate U_i over $(0, T]$, we multiply (3.2) by the integrating factor obtained in (3.3). Then, we obtain:

$$\begin{aligned} U_i e^{(\Phi_i+\Phi_j)t} &= \int_0^T \int_0^T e^{\Phi_i\zeta}\tau_i(\zeta)e^{\Phi_j\eta}\tau_j(\eta)d\zeta d\eta, \\ \Rightarrow U_i &= \int_0^T e^{-\Phi_i(t-\zeta)}\tau_i(\zeta)d\zeta \int_0^T e^{-\Phi_j(t-\eta)}\tau_j(\eta)d\eta, \end{aligned} \tag{3.4}$$

and

$$|U_i|^2 \le \frac{1}{2\,(\Phi_i + \Phi_j)} \int_0^T \int_0^T |\tau_i(\zeta)|^2\, |\tau_j(\eta)|^2 d\zeta d\eta. \tag{3.5}$$

Hence, in the energy norm, for a stable independent variable t, we have:

$$\|\tilde{U}(x, y, t)\|_E^2 \le \sum_{i=1}^{n}\sum_{j=1}^{n} \frac{1}{2}\left(\int_0^T \int_0^T |\tau_i(\zeta)|^2\, |\tau_j(\eta)|^2 d\zeta d\eta\right). \tag{3.6}$$

Therefore, the testing series (2.1) is convergent for a given value of the independent variable t.

Consequently, we obtain:

$$\left(\frac{\partial\tilde{U}}{\partial t}, \xi\right)_0 + \gamma\left(\tilde{U}, \xi\right) = (\phi, \xi)_0\,, \tag{3.7}$$

where $\gamma(\cdot,\cdot)$ and $(\cdot,\cdot)_0$ are the bilinear form and inner product, respectively, as shown in [7, 33]. Now, system (3.7) provides an initial value problem that converges to the exact solution of (1.1). Since it is easier to apply a numerically stable iterative scheme, Eq. (2.7) refers to:

$$\{U\}_{j+1} = [\mathbb{B}]\,\{U\}_j + \mathbb{C}^{-1}\,\{\mathbb{F}\}_j\,. \tag{3.8}$$

Here, $[\mathbb{B}]$ is obtained from the finite element spatial discretization and denotes the system (iteration) matrix, which typically incorporates the assembled stiffness and mass matrices derived from the weak formulation. Additionally, $\{U\}_j$ represents the solution at the present time t, and $\{U\}_{j+1}$ represents the solution at the next time level $(t + \Delta t)$, where the next-step solution $\{U\}_{j+1}$ depends on the present solution $\{U\}_j$. Hence, iterative errors may occur. The iterative scheme becomes unstable due to the unbounded growth of the iterative error, and stable otherwise. Moreover, the necessary and sufficient condition for bounded error will be:

$$([\mathbb{B}] - \alpha_{max}[I])\,\{U\} = 0. \tag{3.9}$$

Here, the eigenvalue problem (3.9) is unconditionally stable. Conversely, it is conditionally stable for any Δt when $\alpha_{\max} \le 1$. The numerical scheme used in this paper is stable and satisfies the compatibility condition (3.10):

$$\Delta t < \frac{2}{(1-2\delta)\alpha_{max}}; \quad \delta < \frac{1}{2}. \tag{3.10}$$

4. Quantification of errors

In this section, we focus on the errors of the proposed numerical scheme, drawing inspiration from the work of Takács (1985) [20, 39]. To complete this task, we assume that U_i and N_i denote the analytical and numerical solutions, respectively. Hence, the approximate absolute error can be evaluated as

$$E_{\text{abs}} = |U_i - N_i|. \tag{4.1}$$

To measure the overall accuracy of the numerical scheme, we compute the total mean square error E_{MSE}, and our subsequent focus is on:

$$E_{\text{MSE}} = \frac{1}{n}\sum_{i=1}^{n}(U_i - N_i)^2. \tag{4.2}$$

Also, the notations $\delta^2(P)$ and $\delta^2(U)$ are used to indicate the sample variance of the analytical and numerical solutions, respectively, as introduced in Eq. (4.3):

$$\delta^2(U) = \frac{1}{n}\sum_{i=1}^{n}(U_i - \bar{U}_i)^2, \quad \delta^2(N) = \frac{1}{n}\sum_{i=1}^{n}(N_i - \bar{N}_i)^2. \tag{4.3}$$

Now, it is more appropriate to expand the sample variance and apply it in the definition of the total mean square error. After completing a straightforward calculation, we obtain:

$$E_{\text{MSE}} = (\delta(U) - \delta(N))^2 + (\bar{U} - \bar{N})^2 + 2(1-\upsilon)\delta(U)\delta(N), \tag{4.4}$$

where

$$\upsilon = \frac{\text{Cov}(U,N)}{\delta(U)\delta(N)}, \quad \text{Cov}(U,N) = \frac{1}{n}\sum U_i N_i - \bar{U}\bar{N}. \tag{4.5}$$

For $\upsilon = 1$,

$$E_{\text{MSE}} = (\delta(U) - \delta(N))^2 + (\bar{U} - \bar{N})^2. \tag{4.6}$$

After a mathematical analysis, we may conclude that in Eq. (4.4), $2(1-\upsilon)\delta(U)\delta(N)$, and $(\delta(U) - \delta(N))^2 + (\bar{U} - \bar{N})^2$ represent the dispersion error and dissipation error, respectively. Moreover, with respect to the L^1 norm, Eq. (4.7) serves as the error measure:

$$E_{\text{num}} = \frac{1}{n}\sum_{i=1}^{n}|U_i - N_i|. \tag{4.7}$$

5. Numerical experiments

In this section, we study two-dimensional linear and nonlinear equations, specifically the two-dimensional Burgers' equation. Through this discussion and the accompanying numerical results, we establish the accuracy and validity of the FEM by demonstrating a strong agreement between the exact and numerical solutions at various time steps. In this study, MATLAB programming has been employed to compute the approximate numerical solutions of the considered problems. The error can be evaluated throughout this section with the help of Eq. (5.1):

$$E = \left|U_j^{\text{exact}} - N_j^{\text{FEM}}\right|. \tag{5.1}$$

Example 5.1. In various fields of applied mathematics, reaction–diffusion equations play a vital role. This type of equation comprises reaction and diffusion terms and, more generally, is used to describe the spread of materials in two-dimensional space. Consequently, it is appropriate to obtain an accurate simulation by considering an efficient numerical method, such as linear FEM. With the above considerations, we introduce a reaction–diffusion equation with the reaction function $f(U(x,y,t)) = e^{-t}\sin(\pi x)\sin(\pi y)(2\pi^2 - 1)$ in the following form:

$$\begin{aligned} U_t = \nabla^2 U + e^{-t}\sin(\pi x)\sin(\pi y)(2\pi^2 - 1),\ (x,y,t) \in \mathcal{D} \equiv \Omega \times (0,T], \\ T > 0,\ \Omega \equiv [0,1]\times[0,1]. \end{aligned} \tag{5.2}$$

TABLE 1. Numerical and analytic solutions of Eq. (5.2).

x	y	$h = \Delta t = 0.0001$			$h = \Delta t = 0.001$			$h = \Delta t = 0.01$		
		FEM	Exact	Error	FEM	Exact	Error	FEM	Exact	Error
0.0000	0.0000	0.0000	0.0000	1.8×10^{-05}	0.0002	0.0000	2.00×10^{-04}	0.0018	0.0000	1.81×10^{-03}
0.1000	0.1000	0.0955	0.0955	9.98×10^{-06}	0.0955	0.0954	1.00×10^{-04}	0.0956	0.0945	1.14×10^{-03}
0.2000	0.2000	0.3455	0.3455	5.42×10^{-06}	0.3451	0.3451	0.00×10^{-04}	0.3414	0.3421	6.08×10^{-04}
0.3000	0.3000	0.6544	0.6544	2.74×10^{-05}	0.6536	0.6539	3.00×10^{-04}	0.6452	0.6480	2.77×10^{-03}
0.4000	0.4000	0.9044	0.9044	4.48×10^{-05}	0.9032	0.9036	4.00×10^{-04}	0.8910	0.8955	4.52×10^{-03}
0.5000	0.5000	0.9998	0.9999	5.15×10^{-05}	0.9985	0.9990	5.00×10^{-04}	0.9849	0.9900	5.20×10^{-03}
0.6000	0.6000	0.9044	0.9044	4.48×10^{-05}	0.9032	0.9036	4.00×10^{-04}	0.8910	0.8955	4.52×10^{-03}
0.7000	0.7000	0.6544	0.6544	2.74×10^{-05}	0.6536	0.6539	3.00×10^{-04}	0.6452	0.6480	2.77×10^{-03}
0.8000	0.8000	0.3455	0.3455	5.42×10^{-06}	0.3451	0.3451	0.00×10^{-04}	0.3414	0.3421	6.08×10^{-04}
0.9000	0.9000	0.0955	0.0955	9.98×10^{-06}	0.0955	0.0954	1.00×10^{-04}	0.0957	0.0945	1.14×10^{-03}
1.0000	1.0000	0.0000	0.0000	1.81×10^{-05}	0.0002	0.0000	2.00×10^{-04}	0.0018	0.0000	1.81×10^{-03}

The corresponding initial and boundary conditions are formulated by Eqs. (5.3) and (5.4) as follows:

$$U(x, y, 0) = \sin(\pi x)\sin(\pi y),\ (x, y) \in \Omega, \tag{5.3}$$

$$\begin{cases} U(0, y, t) = 0.0,\ U(1, y, t) = e^{-t}\sin(\pi)\sin(\pi y),\ t > 0, \\ U(x, 0, t) = 0.0,\ U(x, 1, t) = e^{-t}\sin(\pi x)\sin(\pi),\ t > 0. \end{cases} \tag{5.4}$$

The analytic solution of (5.2) is $U(x, y, t) = e^{-t}\sin(\pi x)\sin(\pi y)$.

Now, to solve Eq. (5.2), we use the formulation derived in Section 2 and obtain Eq. (2.4), $\frac{da_j(t)}{dt}C_{i,j} + K_{i,j}a_j(t) = F_i(t)$, where

$$\begin{cases} K_{i,j} = A_{i,j} + B_{i,j},\quad C_{i,j} = \displaystyle\sum_{j=1}^{n} \iint_e \psi_i(x)\psi_j(x)\psi_i(y)\psi_j(y)dxdy, \\ A_{i,j} = \displaystyle\iint_e \left[\frac{d\psi_i}{dx}\sum_{j=1}^{n}\frac{d\psi_j(x)}{dx}\psi_j(y)\right]\psi_i(y)dxdy,\quad B_{i,j} = \iint_e \left[\frac{d\psi_i}{dy}\sum_{j=1}^{n}\frac{d\psi_j(y)}{dy}\psi_j(x)\right]\psi_i(x)dxdy, \end{cases}$$

and Eq. (5.5) can be used to obtain $F_i(t)$ as follows:

$$\begin{cases} F_i(t) = L_i(t) + R_i(t), \\ L_i(t) = \displaystyle\int_e \left[\tilde{U}_x\psi_i(x)\right]_e \psi_i(y)dy + \int_e \left[\tilde{U}_y\psi_i(y)\right]_e \psi_i(x)dx, \\ R_i(t) = \displaystyle\iint_e e^{-t}\sin(\pi x)\sin(\pi y)(2\pi^2 - 1)\psi_i(x)\psi_i(y)dxdy. \end{cases} \tag{5.5}$$

Proceeding with a straightforward computation, as in the derivation of the weak formulation, we obtain the following final system:

$$CU_{j+1} + (K\Delta t - C)U_j = F\Delta t. \tag{5.6}$$

Eventually, we obtain the numerical solution of (5.2) by applying row and column operations to the above system (5.6). Accordingly, we may conclude that the approximate numerical solution of (5.2), obtained using the linear FEM with a number of elements $n = 10$ and linear basis functions (2.3), is presented in Table 1 for several time steps $h = \Delta t$, as well as for the steady-state results.

In this context, the numerical results of (5.2) are presented in Table 1, while the error analysis is provided in Table 2. These results strongly support the accuracy and validity of the proposed linear FEM scheme. The findings of this study are also illustrated graphically in Figures 1 and 2.

In this study, Tables 3 and 4 provide a comparative analysis among linear FEM, quadratic FEM [26], and FDM. Table 3 demonstrates that all three methods yield nearly identical numerical accuracy, indicating the reliability of each

TABLE 2. Error analysis of numerical result of Eq. (5.2).

h	E_{num}	Dissipation Error	Dispersion Error	Total Error
10^{-4}	2.6302×10^{-5}	9.2751×10^{-10}	9.9977×10^{-2}	9.9977×10^{-2}
10^{-3}	2.6683×10^{-4}	9.3561×10^{-8}	9.9770×10^{-2}	9.9771×10^{-2}
10^{-2}	2.6926×10^{-3}	9.5229×10^{-6}	9.7721×10^{-2}	9.7730×10^{-2}

TABLE 3. Comparison between linear FEM, quadratic FEM and FDM solutions of Eq. (5.2).

x	Linear FEM with fixed $y = 0.5$			Quadratic FEM with fixed $y = 0.5$			FDM with fixed $y = 0.5$		
	FEM_{Linear}	Exact	Error	$FEM_{Quadratic}$	Exact	Error	FDM	Exact	Error
0.0	1.8×10^{-5}	0.0000	1.8×10^{-5}	0.0009	0.0000	8.5×10^{-4}	0.0009	0.0000	9.2×10^{-4}
0.5	0.9998	0.9999	5.1×10^{-5}	0.9998	0.9999	4.3×10^{-5}	0.9997	0.9999	2.0×10^{-4}
1.0	1.8×10^{-5}	1.2×10^{-16}	1.8×10^{-5}	0.0003	1.2×10^{-16}	2.9×10^{-4}	0.0004	1.2×10^{-16}	3.5×10^{-4}

TABLE 4. CPU time and maximum error of linear FEM, quadratic FEM and FDM solutions of Eq. (5.2).

	FEM_{Linear}	$FEM_{Quadratic}$	FDM
CPU (Seconds)	0.494	1.329	2.085
Max Error	1.5×10^{-1}	2.4×10^{-1}	7.8×10^{-1}

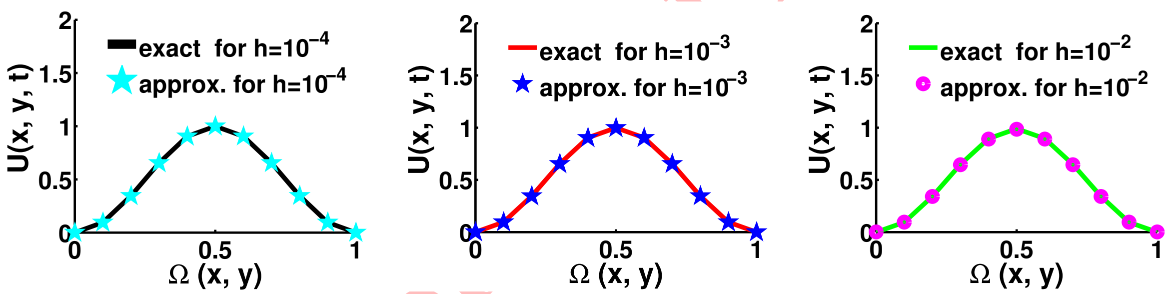

FIGURE 1. Numerical and analytic solutions of Eq. (5.2) for different time steps, $h = \Delta t$.

approach. However, the computational efficiency differs significantly. As shown in Table 4, the linear FEM requires substantially less CPU time compared to both quadratic FEM and FDM. This reduction in computational cost arises from the simpler formulation and lower complexity of linear basis functions. Therefore, despite achieving comparable accuracy, the linear FEM proves to be more efficient and computationally economical, making it a preferable choice for solving two-dimensional CDR problems.

To verify the precise agreement between the numerical and steady-state solutions, we include Figure 3, which presents a comprehensive comparative analysis along with an error map for Eq. (5.2). This graphical depiction not only facilitates an in-depth comparison but also highlights the negligible magnitude of the error, even for the very small time step $h = 10^{-4}$. In essence, the linear FEM demonstrates its ability to provide accurate results, thereby reinforcing its suitability for CDR models.

We also study the behavior of the proposed method for a larger final time $T = 10$, and the corresponding results are shown in Figure 4. When we compare this with Figure 1, where a smaller final time is considered, we observe a clear difference in accuracy. For the smaller final time, the numerical solution matches very well with the exact solution and shows good agreement for different time step sizes. However, for $T = 10$, the error becomes noticeably larger in all cases, which indicates that the accuracy decreases as the final time increases. This is mainly due to the accumulation

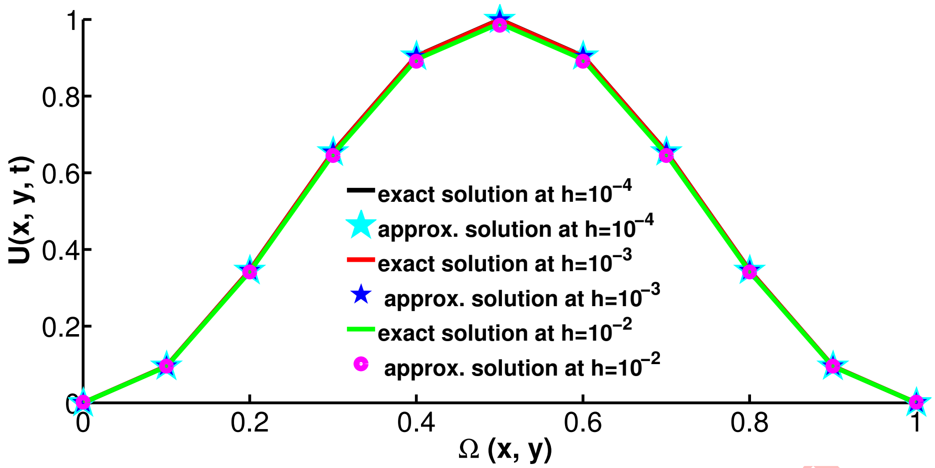

Figure 2. Similarity between numerical and analytic solutions of Eq. (5.2) for different time steps h.

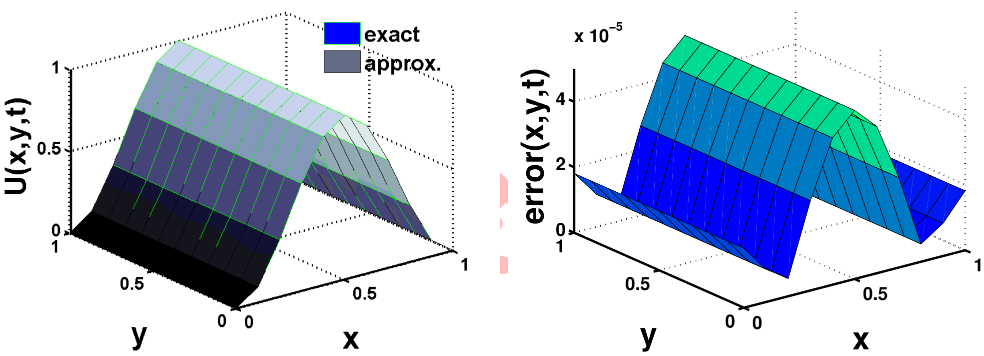

Figure 3. Comparative analysis and error map of Eq. (5.2) for $h = 10^{-4}$.

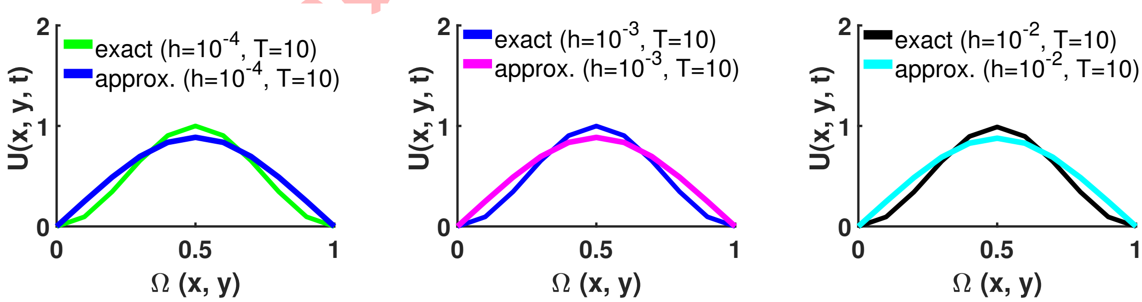

Figure 4. Comparison at total time $T = 10$ for Eq. (5.2) with different time steps $h = \Delta t$.

of time discretization error over long-time integration. From this comparison, we may conclude that the proposed method performs well for short-time simulations, but the accuracy gradually reduces for larger final times, although the overall behavior of the solution remains consistent. We also observe that spatial discretization has a significant effect on the accuracy of the numerical solution. For smaller final times, a relatively coarse mesh with fewer elements is sufficient to obtain accurate results. On the other hand, for larger final times, a finer mesh with a greater number of elements is required to maintain accuracy and to properly control the accumulated error.

Example 5.2. The Fisher–KPP equation, also referred to as the Fisher–Kolmogorov–Petrovsky–Piskunov equation, is a two-dimensional PDE commonly employed to describe the spatiotemporal evolution of population density or similar quantities. This reaction–diffusion equation has widespread applications in ecological, biological, and other scientific domains. Renowned for its ability to capture phenomena such as the diffusion of biological populations and the propagation of fronts in reaction–diffusion systems, the Fisher–KPP equation exhibits a transition from localized initial conditions to propagating wave solutions that travel through space. Its study is well established in the field of mathematical biology, and it is named after its contributors: Ronald A. Fisher, Andrey Kolmogorov, Igor Petrovsky, and Nikolai Piskunov. Moreover, the Fisher–KPP equation takes the following general form in two spatial dimensions:

$$\begin{cases} U_t = C_0\nabla^2 U + \gamma U(1-U),\ (x,y,t)\in\mathcal{D}\equiv\Omega\times(0,T], T>0,\ \ \Omega\equiv[a_1,a_2]\times[b_1,b_2],\\ U(x,y,0)=U_0(x,y);\ (x,y)\in\Omega,\\ U(a_1,y,t)=q_1(y,t),\ U(a_2,y,t)=q_2(y,t),\ t>0,\\ U(x,b_1,t)=q_3(x,t),\ U(x,b_2,t)=q_4(x,t),\ t>0. \end{cases} \tag{5.7}$$

With the diffusion coefficient set to $C_0 = 1$ and the growth rate $\gamma = 1$, the equation takes the following form:

$$U_t = \nabla^2 U + U(1-U),\ (x,y,t)\in\mathcal{D}\equiv\Omega\times(0,T]\,,\ \Omega\equiv[0,1]\times[0,1],\ T>0. \tag{5.8}$$

The initial condition is performed by (5.9):

$$U(x,y,0)=\left[\frac{1}{2}-\frac{1}{2}\tanh\left(\frac{1}{4}\sqrt{\frac{1}{3}}(x+y)\right)\right]^2,\ (x,y)\in\Omega\equiv[0,1]\times[0,1]. \tag{5.9}$$

Correspondingly, the boundary conditions for Eq. (5.8) are given by:

$$\begin{cases} U(0,y,t)=\left[\frac{1}{2}-\frac{1}{2}\tanh\left(\frac{1}{4}\sqrt{\frac{1}{3}}y-5\sqrt{\frac{1}{3}}t\right)\right]^2,\\ U(1,y,t)=\left[\frac{1}{2}-\frac{1}{2}\tanh\left(\frac{1}{4}\sqrt{\frac{1}{3}}(1+y)-5\sqrt{\frac{1}{3}}t\right)\right]^2,\\ U(x,0,t)=\left[\frac{1}{2}-\frac{1}{2}\tanh\left(\frac{1}{4}\sqrt{\frac{1}{3}}x-5\sqrt{\frac{1}{3}}t\right)\right]^2,\\ U(x,1,t)=\left[\frac{1}{2}-\frac{1}{2}\tanh\left(\frac{1}{4}\sqrt{\frac{1}{3}}(1+x)-5\sqrt{\frac{1}{3}}t\right)\right]^2,\ t>0. \end{cases} \tag{5.10}$$

The corresponding exact solution of Eq. (5.8) is given by:

$$U(x,y,t)=\left[\frac{1}{2}-\frac{1}{2}\tanh\left(\frac{1}{4}\sqrt{\frac{1}{3}}(x+y)-5\sqrt{\frac{1}{3}}t\right)\right]^2,\ (x,y,t)\in\mathcal{D}\equiv\Omega\times(0,T],\ T>0.$$

To move forward, we utilize a solution approach similar to that used in Example 5.1 to derive the matrix form (2.4). It is important to note that all coefficients remain unchanged, except for $F_i(t)$. Moreover, $F_i(t)$ can be incorporated using the following Eq. (5.11):

$$\begin{cases} F_i(t)=L_i(t)+R_i(t),\\ L_i(t)=\int\limits_e \left[\tilde{U}_x\psi_i(x)\right]_e\psi_i(y)dy+\int\limits_e \left[\tilde{U}_y\psi_i(y)\right]_e\psi_i(x)dx,\\ R_i(t)=\iint_e f(\tilde{U}(x,y,t))\psi_i(x)\psi_i(y)dxdy. \end{cases} \tag{5.11}$$

Table 5. Approximate and exact solution of 2D Fisher-KPP Eq. (5.8).

x	y	$h=\Delta t=0.00001$			$h=\Delta t=0.0001$			$h=\Delta t=0.001$		
		FEM	Exact	Error	FEM	Exact	Error	FEM	Exact	Error
0.0000	0.0000	0.2500	0.2500	2.0×10^{-05}	0.2497	0.2497	2.0×10^{-04}	0.2466	0.2471	2.0×10^{-03}
0.1000	0.1000	0.2357	0.2358	3.4×10^{-05}	0.2354	0.2355	3.4×10^{-04}	0.2322	0.2330	3.5×10^{-03}
0.2000	0.2000	0.2220	0.2220	2.8×10^{-05}	0.2217	0.2217	2.8×10^{-04}	0.2187	0.2193	2.9×10^{-03}
0.3000	0.3000	0.2086	0.2086	2.5×10^{-05}	0.2084	0.2084	2.5×10^{-04}	0.2055	0.2060	2.5×10^{-03}
0.4000	0.4000	0.1958	0.1958	2.1×10^{-05}	0.1955	0.1956	2.1×10^{-04}	0.1929	0.1933	2.1×10^{-03}
0.5000	0.5000	0.1834	0.1834	1.6×10^{-05}	0.1832	0.1832	1.6×10^{-04}	0.1807	0.1810	1.7×10^{-03}
0.6000	0.6000	0.1716	0.1716	1.2×10^{-05}	0.1713	0.1714	1.2×10^{-04}	0.1690	0.1692	1.2×10^{-03}
0.7000	0.7000	0.1602	0.1602	6.8×10^{-06}	0.1600	0.1600	6.8×10^{-05}	0.1578	0.1580	7.0×10^{-04}
0.8000	0.8000	0.1494	0.1494	1.9×10^{-06}	0.1492	0.1492	1.9×10^{-05}	0.1472	0.1472	2.0×10^{-04}
0.9000	0.9000	0.1391	0.1391	5.7×10^{-06}	0.1389	0.1389	5.6×10^{-05}	0.1370	0.1369	5.0×10^{-04}
1.0000	1.0000	0.1292	0.1293	6.4×10^{-06}	0.1291	0.1291	6.5×10^{-05}	0.1271	0.1272	7.0×10^{-04}

Table 6. Error analysis of approximate solution of 2D Fisher-KPP Eq. (5.8).

h	E_{num}	Dissipation Error	Dispersion Error	Total Error
10^{-5}	1.7592×10^{-5}	1.7959×10^{-11}	1.6729×10^{-2}	1.6729×10^{-2}
10^{-4}	1.7648×10^{-4}	1.8018×10^{-9}	1.6700×10^{-2}	1.6700×10^{-2}
10^{-3}	1.8000×10^{-3}	1.8617×10^{-7}	1.6300×10^{-2}	1.6300×10^{-2}

After simplification, we obtain the final system as shown in Eq. (5.12):

$$CU_{j+1}+(K\Delta t-C)U_j=F\Delta t. \tag{5.12}$$

Therefore, by incorporating a suitable iterative approach to simplify these direct computations, we obtain the numerical solution of Eq. (5.8) over different time intervals within the two spatial domains. This leads to the presentation of the corresponding results in Table 5.

Table 7. Comparison between linear FEM, quadratic FEM and FDM solutions of Fisher-KPP Eq. (5.8).

x	Linear FEM with fixed $y=0.5$			Quadratic FEM with fixed $y=0.5$			FDM with fixed $y=0.5$		
	FEM_{Linear}	Exact	Error	$FEM_{Quadratic}$	Exact	Error	FDM	Exact	Error
0.0	2.12×10^{-1}	2.13×10^{-1}	1.3×10^{-3}	2.26×10^{-1}	2.13×10^{-1}	1.4×10^{-2}	2.13×10^{-1}	2.13×10^{-1}	1.3×10^{-3}
0.5	1.78×10^{-1}	1.78×10^{-1}	3.2×10^{-4}	1.79×10^{-1}	1.78×10^{-1}	9.3×10^{-4}	1.79×10^{-1}	1.78×10^{-1}	5.2×10^{-4}
1.0	1.52×10^{-1}	1.53×10^{-1}	1.1×10^{-3}	1.64×10^{-1}	1.53×10^{-1}	1.2×10^{-2}	1.52×10^{-1}	1.53×10^{-1}	9.6×10^{-2}

Table 8. CPU time and maximum error of linear FEM, quadratic FEM and FDM solutions of Fisher-KPP Eq. (5.8).

	FEM_{Linear}	$FEM_{Quadratic}$	FDM
CPU (Second)	0.021	1.794	3.055
Max Error	1.1×10^{-2}	1.1×10^{-2}	1.4×10^{-2}

Upon reviewing the contents of Table 5, it becomes apparent that the proposed numerical scheme yields improved accuracy over the two spatial domains, even for different time increments $h=\Delta t$. A notable agreement is observed between the approximate and exact solutions. The relevant information derived from the formulation is visually represented in Figures 5 and 6. By examining these results, we observe the relationship between the two solutions at various time steps h. It is reasonable to neglect the error term in this context, indicating the accuracy and validity of the newly implemented numerical scheme. However, for larger time steps, the error becomes more noticeable compared to the case of smaller time steps. For a more detailed illustration, three-dimensional surface plots are

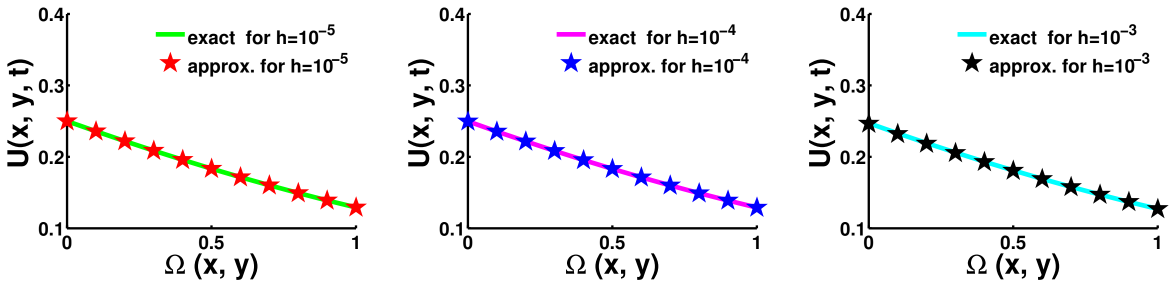

FIGURE 5. Approximate and exact solution of 2D Fisher-KPP Eq. (5.8) for several time steps, h.

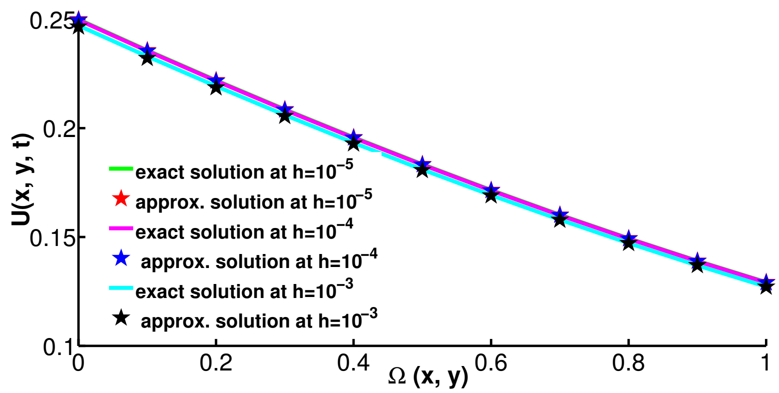

FIGURE 6. Plot of the correlative study between approximate and exact solution of 2D Fisher-KPP Eq. (5.8) for several time steps, h.

presented in Figures 7 and 8, where the first shows the approximate and exact solutions for a fixed time step, and the second presents the error map comparing the approximate and exact solutions. Ultimately, these figures confirm the suitability of the linear FEM approach for solving two-dimensional parabolic PDEs and demonstrate its rapid convergence for Eq. (5.8). Additionally, Table 6 presents the error analysis of the approximate solution for the two-dimensional Fisher–KPP Eq. (5.8), further confirming the effectiveness of the method.

In Example 5.2, we also present two additional Tables 7 and 8 to further examine the performance of the proposed numerical scheme. The first table shows the comparison between linear FEM, quadratic FEM [26], and FDM in terms of accuracy, and the second one presents the comparison in terms of computational cost and maximum error. From these comparisons, it is observed that all three methods provide almost similar accuracy, while differences appear in computational efficiency. The second table provides the comparison of CPU time and maximum error, which again shows similar behavior in the sense of accuracy for all methods. However, for CPU time, linear FEM performs better with lower computational cost compared to both quadratic FEM and FDM solutions. From these results, we may conclude that although all methods give comparable accuracy, the linear FEM is more efficient due to its lower CPU time requirement.

In the same Example 5.2, we have computed the linear FEM solution for three different time steps at total time $T = 10$ to investigate the limiting behavior of the model and to understand its applicability for larger final times, as represented visually in Figure 9. From Figure 9, we observe that, for larger final times, the error increases compared to that of smaller final times. This indicates that the accumulation of discretization error becomes more significant as time progresses. However, the overall behavior of the numerical solution remains stable and consistent with the

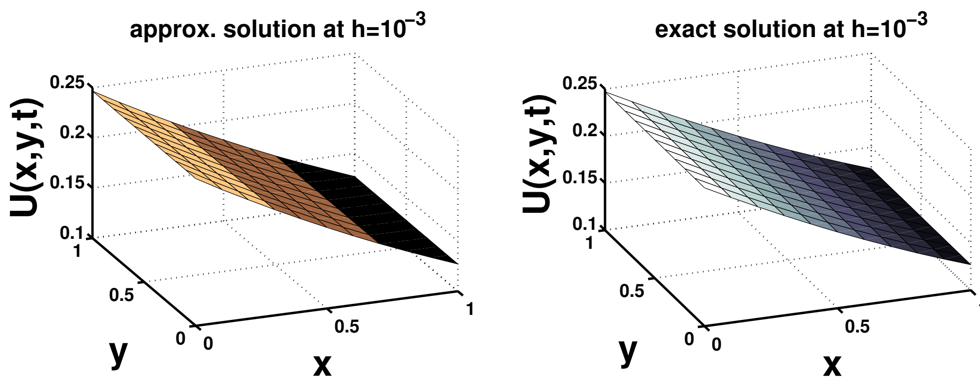

FIGURE 7. Plot of approximate and exact solution of 2D Fisher-KPP Eq. (5.8) for $h = 10^{-3}$.

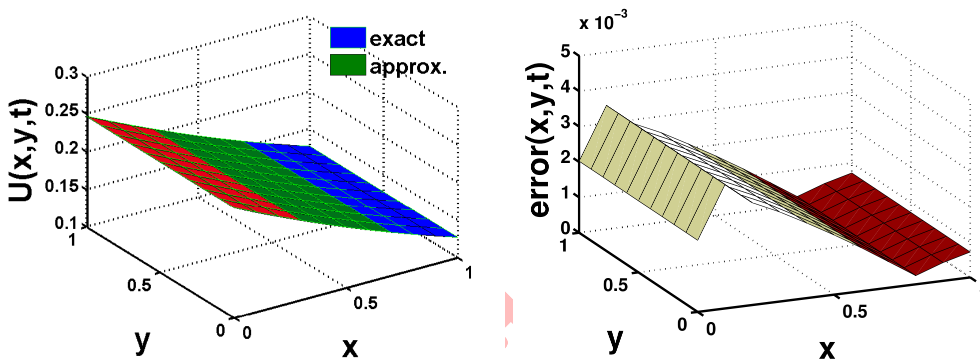

FIGURE 8. Relationship between the approximate and exact solutions and error analysis of the 2D Fisher-KPP Eq. (5.8) for $h = 10^{-3}$.

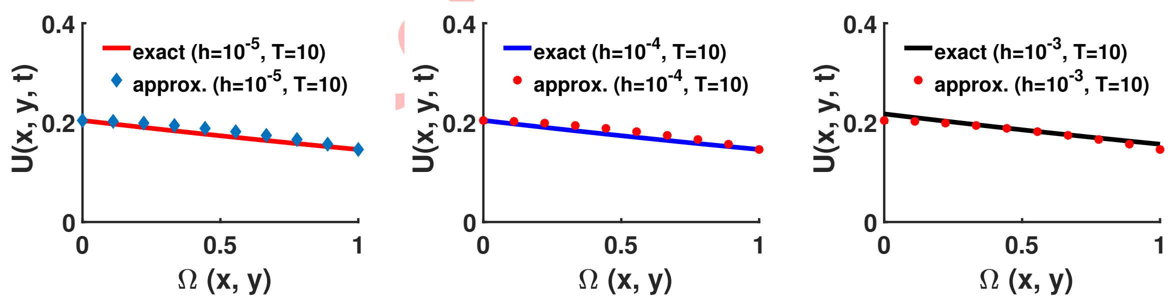

FIGURE 9. Correlative study at total time, $T = 10$ of Fisher-KPP Eq. (5.8) for several time steps, h.

expected physical nature of the model. Therefore, although the accuracy slightly deteriorates for larger final times, the proposed method still preserves the qualitative behavior of the solution and remains reliable for long-time simulations.

Example 5.3. In Section 5, we have discussed three boundary value problems. Among them, the first one is a two-dimensional linear reaction–diffusion model, whereas the last two examples are two-dimensional nonlinear CDR models. From both theoretical and practical points of view, nonlinear CDR problems generally arise when physical processes in different scientific fields are modeled. Since the main purpose of the present work is to ensure the reliability and validity of linear FEM for solving two-dimensional CDR models, it is more appropriate to introduce the nonlinear CDR model (5.13) with reaction term $f(U(x,y,t)) = 0$, known as the two-dimensional Burgers' equation [27], with suitable initial and boundary conditions. This model exhibits rapid convergence and good accuracy.

The Burgers' equation is a fundamental nonlinear PDE arising in fluid mechanics. It appears in various areas of applied mathematics, including the modeling of dynamical systems, heat conduction, and acoustic wave propagation [8, 32]. It is widely used to describe physical phenomena such as mass transport, shock wave formation, turbulence, boundary layer behavior, as well as problems in climate dynamics, atmospheric pressure, meteorology, commuter traffic flow, and acoustic transmission. Furthermore, two dimensional Burger's equation have a great specification for exploring the waves in near-surface water and dynamic mechanism of gas. Also, it is a equation which contains the effects of nonlinear propagation and diffusion. Because of it's great use, many researchers are interested to evaluate the solution of this equation by various techniques. Here, as numerical technique, our work acts with linear FEM.

$$\begin{cases} U_t + U\,\nabla U = \mu \nabla^2 U,\ (x,y,t) \in \mathcal{D} \equiv \Omega \times (0,T], T > 0,\ \ \Omega \equiv [w_1, w_2] \times [w_3, w_4], \\ U(x,y,0) = U_0(x,y),\ (x,y) \in \Omega, \\ U(w_1,y,t) = v_1(y,t),\ U(w_2,y,t) = v_2(y,t),\ t > 0, \\ U(x,w_3,t) = v_3(x,t),\ U(x,w_4,t) = v_4(x,t),\ t > 0. \end{cases} \tag{5.13}$$

In this example, $U = U(x,y,t)$ represents the velocity, $\mu = \frac{1}{Re} > 0$ denotes the coefficient of kinematic viscosity, and Re is the Reynolds number. The functions U_0, v_1, v_2, v_3, and v_4 are smooth functions. Here, U_t represents the unsteady term, $U\,\nabla U$ denotes the nonlinear convective term, and $\mu\nabla^2 U$ represents the diffusive term. To understand the applicability of Burgers' equation in different fields such as anthropology, technology, and industrial science, we consider the two-dimensional Burgers' equation over the domain $\Omega = [0,1] \times [0,1]$ with $Re = 100$, which takes the form (5.14):

$$U_t + U\,\nabla U = \frac{1}{Re}\ \nabla^2 U,\ (x,y,t) \in \mathcal{D} \equiv \Omega \times (0,T],\ T > 0. \tag{5.14}$$

The initial condition is given by Eq. (5.15):

$$U(x,y,0) = \frac{1}{1 + e^{\frac{Re(x+y)}{2}}},\ (x,y) \in \Omega. \tag{5.15}$$

Correspondingly, the boundary conditions for Eq. (5.14) are given by:

$$\begin{cases} U(0,y,t) = \frac{1}{1+e^{\frac{Re(y-t)}{2}}},\ U(1,y,t) = \frac{1}{1+e^{\frac{Re(1+y-t)}{2}}},\ t > 0, \\ U(x,0,t) = \frac{1}{1+e^{\frac{Re(x-t)}{2}}},\ U(x,1,t) = \frac{1}{1+e^{\frac{Re(1+x-t)}{2}}},\ t > 0. \end{cases} \tag{5.16}$$

Moreover, the exact solution of Eq. (5.14) is given by:

$$U(x,y,t) = \frac{1}{1 + e^{\frac{Re(x+y-t)}{2}}},\ (x,y,t) \in \mathcal{D} \equiv \Omega \times (0,T],\ T > 0.$$

Let us evaluate the numerical solution of this two-dimensional nonlinear Burgers' equation at the time level $t = 0.25$ for different time steps $h = \Delta t = 0.001,\ 0.1$. To obtain the approximate linear FEM solution of (5.14), we consider a finite number of elements, $n = 10$, along with linear basis functions (2.3). Afterwards, we complete the weak formulation process of linear FEM for the two-dimensional nonlinear CDR model. Since, Eq. (5.14) involves a nonlinear convection term, to handle this computational complexity, we use an initial approximation based on the initial condition and subsequently obtain the associated coefficients.

Hence, after appropriate simplification, following the weak formulation derived in Section 2, we obtain the final system:

$$CU_{j+1} + (K\Delta t - C)U_j = F\Delta t. \tag{5.17}$$

Solving this system using a suitable iterative method in MATLAB, we obtain the approximate linear FEM solution, which is presented in Table 9.

Table 9. Approximate and exact solutions of the 2D Burgers' Eq. (5.14).

x	y	$h = \Delta t = 0.001$			$h = \Delta t = 0.1$		
		FEM	Exact	Error	FEM	Exact	Error
0.0	0.0	0.999418956478526	0.999996273360716	0.000577316882190	0.951795647852624	0.999996273360716	0.048200625508092
0.1	0.1	0.923655441485895	0.924141819978757	0.000486378492861	0.879644148589504	0.924141819978757	0.044497671389252
0.2	0.2	0.000499741499313	0.000499741499313	0.000053037137610	0.000474149931342	0.000552778636924	0.000078628705582
0.3	0.3	0.000000002272098	0.000552778636924	0.000000022837893	0.000000227209760	0.000000025109991	0.000000202099769
0.4	0.4	0.000000000288594	0.000000025109991	0.000000000289734	0.000000028859423	0.000000000001140	0.000000028860563
0.5	0.5	0.000000000036656	0.000000000001140	0.000000000036656	0.000000003665627	0.000000000000000	0.000000003665627
0.6	0.6	0.000000000004656	0.000000000000000	0.000000000004656	0.000000000465596	0.000000000000000	0.000000000465596
0.7	0.7	0.000000000000591	0.000000000000000	0.000000000000591	0.000000000059139	0.000000000000000	0.000000000059139
0.8	0.8	0.000000000000075	0.000000000000000	0.000000000000075	0.000000000007514	0.000000000000000	0.000000000007514
0.9	0.9	0.000000000000010	0.000000000000000	0.000000000000010	0.000000000000969	0.000000000000000	0.000000000000969
1.0	1.0	0.000000000000002	0.000000000000000	0.000000000000002	0.000000000000242	0.000000000000000	0.000000000000242

Table 10. Error analysis of approximate solution of 2D Burgers' Eq. (5.14).

h	E_{num}	Dissipation Error	Dispersion Error	Total Error
10^{-3}	1.1168×10^{-4}	5.8144×10^{-8}	1.4809×10^{-2}	1.4809×10^{-2}
10^{-2}	9.4494×10^{-4}	4.5104×10^{-6}	1.4745×10^{-2}	1.4750×10^{-2}
10^{-1}	9.2777×10^{-3}	4.3894×10^{-4}	1.4103×10^{-2}	1.4542×10^{-2}

Table 11. Spatial errors with identical time and fixed time step of 2D Burgers' Eq. (5.14).

Spatial errors with fixed $T = 0.0001$ and $\Delta t = \frac{T}{5}$	
Linear FEM Scheme	
Grid Points, P	Spatial Errors
$\frac{1}{10}$	4.5625×10^{-5}
$\frac{1}{5}$	2.0715×10^{-9}
$\frac{3}{10}$	9.4000×10^{-14}
$\frac{2}{5}$	0.0000×10^{-15}
$\frac{1}{2}$	0.0000×10^{-15}

Table 12. Temporal errors with identical time at fixed grid point of 2D Burgers' Eq. (5.14).

Temporal errors with fixed $T = 1$ and grid point, P $= \frac{1}{5}$	
Linear FEM Scheme	
Time Steps	Temporal errors
$\frac{T}{10}$	3.0590×10^{-7}
$\frac{T}{5}$	4.5398×10^{-5}
$\frac{3T}{10}$	6.6929×10^{-3}
$\frac{2T}{5}$	5.0000×10^{-1}
$\frac{T}{2}$	9.9331×10^{-1}

Following this, a thorough mathematical analysis is performed on the tabulated results presented in Table 9. The results clearly demonstrate strong agreement between the approximate solution obtained through the linear FEM and the established solution reported in the literature [27]. To further support this observation, Table 10 presents an error analysis of the numerical solutions for Eq. (5.14), thereby highlighting the stability of the proposed linear FEM method. The spatial errors and convergence rates are provided in Table 11. We observe a consistent second-order spatial convergence.

Importantly, Tables 11 and 12 present the spatial errors for uniform time instances with $T = 0.0001$ and a constant time step $\Delta t = \frac{T}{5}$ over different grid points, as well as for a fixed grid point $P = \frac{1}{5}$ with varying time steps for $T = 1$. These tabulated results help in assessing the accuracy of the proposed technique across different time intervals and spatial grid configurations.

TABLE 13. Comparison between linear FEM, quadratic FEM and FDM solutions of Burgers' Eq. (5.14).

x	Linear FEM			Quadratic FEM			FDM		
	FEM_{Linear}	Exact	Error	$FEM_{Quadratic}$	Exact	Error	FDM	Exact	Error
0.0	0.9999	0.9999	1.0×10^{-4}	-0.3775	-0.4999	0.1225	0.9998	0.9999	1.0×10^{-4}
0.5	3.67×10^{-13}	0.0000	4.03×10^{-12}	-0.6101	-0.5622	0.0479	1.2×10^{-6}	0.0000	1.2×10^{-6}
1.0	0.0000	0.0000	0.0000	-0.6225	-0.6225	0.0000	0.0000	0.0000	0.0000

TABLE 14. CPU time and maximum error of linear FEM, quadratic FEM and FDM of Burgers' Eq. (5.14).

	FEM_{Linear}	$FEM_{Quadratic}$	FDM
CPU (Second)	0.0092	0.0126	0.0166
Max Error	1.1×10^{-4}	$1.2\ \times10^{-1}$	4.3×10^{-2}

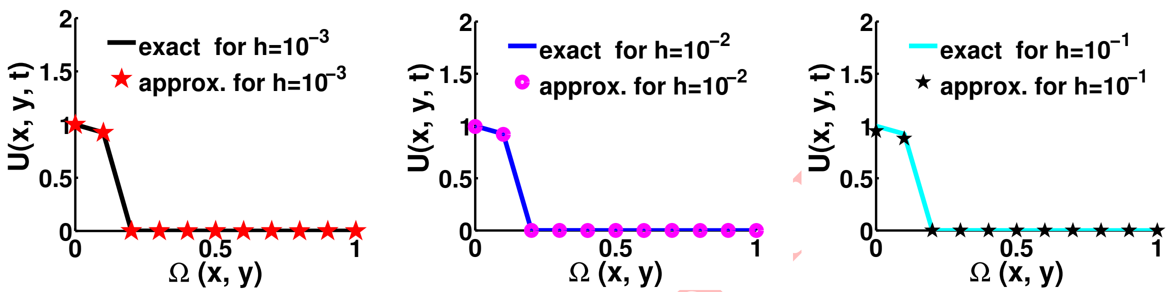

FIGURE 10. Approximate and exact solution of 2D Burgers' Eq. (5.14).

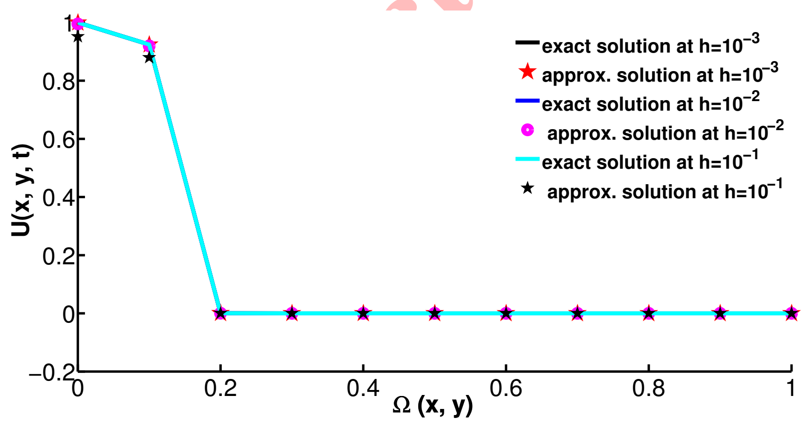

FIGURE 11. Correlation plot of the comparative study between the approximate and exact solutions of 2D Burgers' Eq. (5.14).

In Table 13, we present a comparison of the linear FEM with quadratic FEM [26] and FDM, similar to the previous Examples 5.1 and 5.2. Additionally, Table 14 provides a comparison of CPU time and maximum error. The findings are consistent with those observed in the earlier examples. It is evident that all three methods provide nearly similar accuracy; however, the linear FEM shows comparable accuracy while requiring significantly lower CPU time compared to quadratic FEM and FDM, demonstrating better computational efficiency and consistency. Therefore, from these comparisons, we conclude that the linear FEM is more efficient while maintaining reliable accuracy.

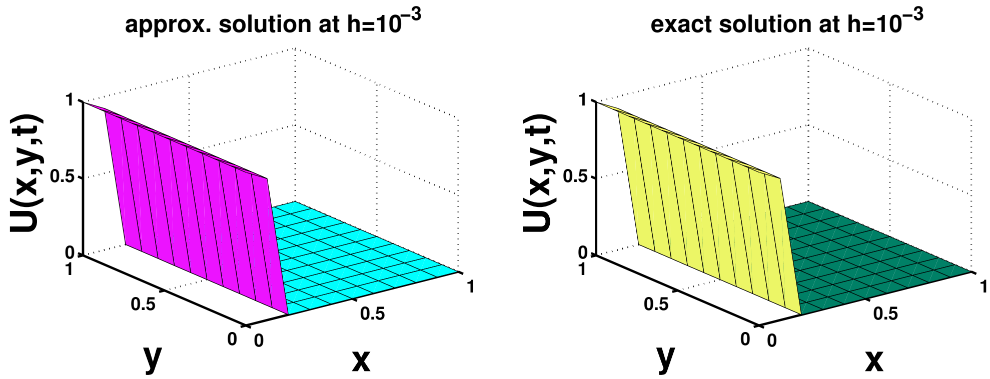

Figure 12. Plot of approximate and exact solution of 2D Burgers' Eq. (5.14) for $h = 10^{-3}$.

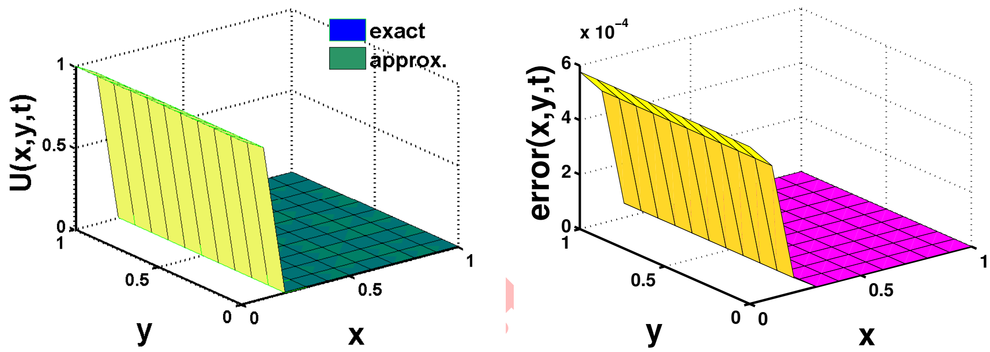

Figure 13. Relation between approximate and exact solution of 2D Burgers' Eq. (5.14) and error map for $h = 10^{-3}$.

In a visual context, Figures 10 and 11 reflect the same observations obtained from Tables 9 and 10. To further validate the accuracy and reliability of the proposed linear FEM approach, we also present three-dimensional plots in Figures 12 and 13. These plots confirm a strong agreement between the approximate and exact solutions, while the associated error remains negligible.

In summary, the linear FEM approach demonstrates strong performance and effectiveness in solving the two-dimensional Burgers' equation. As a result, the proposed scheme shows potential for solving a wide range of two-dimensional nonlinear parabolic PDEs.

In Figure 14, we present a graphical comparison between the exact and approximate solutions at total time $T = 10$ for Example 5.3. The figure clearly shows that, for higher final time, the accuracy decreases, which indicates a limiting behavior of the proposed method. This observation is consistent with the results obtained in the previous two examples. However, the method still demonstrates good reliability when smaller time steps are used. On the other hand, for larger time steps, the accuracy deteriorates and the method does not perform well. Therefore, the proposed scheme remains effective for sufficiently small time steps even at larger final times.

6. Conclusion

Within the context of our ongoing investigation, we have formulated the weak form of linear FEM to address spatially two-dimensional parabolic PDEs. In this study, we consider three illustrative cases. The first case deals with a two-dimensional linear reaction–diffusion equation, the second involves a non–linear reaction–diffusion equation

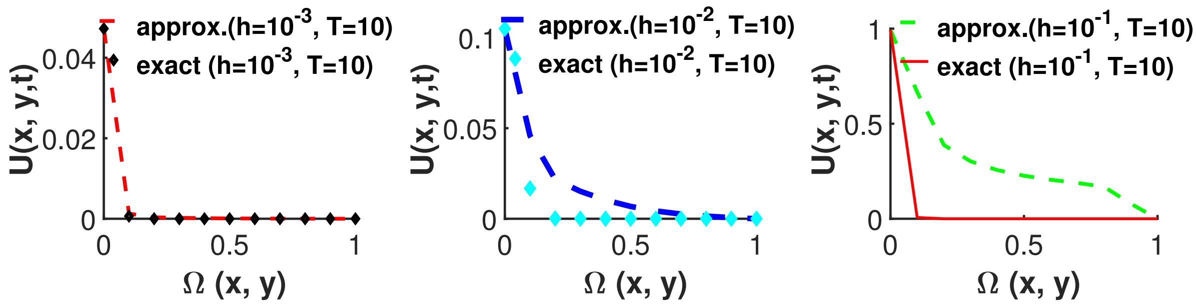

Figure 14. Correlative study at total time, T=10 of 2D Burgers' Eq. (5.14).

(Fisher–KPP equation), and the final case corresponds to a two-dimensional Burgers' equation. In all cases, the approximate solutions exhibit rapid convergence towards the corresponding exact solutions. This approach generates numerical solutions of satisfactory accuracy, supported by negligible errors observed in the error analysis. A good agreement between the approximate and exact solutions is further confirmed through organized data and graphical representations. The proposed method produces consistent and accurate results, providing strong evidence of its effectiveness. In conclusion, the proposed linear FEM formulation demonstrates accuracy, efficiency, and reliability due to its simple weak formulation, computational efficiency, and ease of implementation. Therefore, the method is effective for solving two-dimensional parabolic PDEs as well as CDR models.

Acknowledgements

The author Sadia Akter Lima acknowledged to the Noakhali Science and Technology University Research Cell (NSTURC) for partial funding support for this project.

Declaration of competing interest

The authors declare no competing interests.

Data Availability statement

Data sharing not applicable to this article as no datasets were generated or analysed during the current study.

Ethical approval

N/A.

Author Contributions (CRediT)

Sadia Akter Lima: Conceptualization, Data curation, Formal analysis, Methodology, Software, Validation, Visualization, Funding acquisition, Writing– original draft.
Md. Shafiqul Islam: Methodology, Investigation, Software, Resources, Project Administration, Writing– review & editing.
Runchang Lin: Methodology, Investigation, Software, Resources, Writing– review & editing.
Md. Kamrujjaman: Conceptualization, Formal analysis, Methodology, Validation, Software, Supervision, Writing– original draft.
All authors have read and agreed to the published version of the manuscript.

References

[1] M. Abbaszadeh, A. Ghoreyshi, and M. Dehghan, *A finite block method framework for nonlinear fractional integro-differential equations*, Mathematical Methods in the Applied Sciences, *49*(4) (2025), 2170–2188.

[2] H. Ali, M. Kamrujjaman, and M. S. Islam, *Numerical computation of FitzHugh-Nagumo equation: A novel galerkin finite element approach*, International Journal of Mathematical Research, *9*(1) (2020), 20–27.

[3] H. Ali, M. Kamrujjaman, and A. Shirin, *Numerical solution of a fractional order Bagley-Torvik equation by quadratic finite element method*, Journal of Applied Mathematics and Computing, *66* (2020), 1–17.

[4] H. Ali, T. Datta, and M. Kamrujjaman, *Efficient family of iterative methods for solving nonlinear simultaneous equations: A comparative study*, Journal of Applied Mathematics and Computation, *5*(4) (2021), 331–337.

[5] H. Ali, M. Kamrujjaman, and M. S. Islam, *An advanced galerkin approach to solve the nonlinear reaction-diffusion equations with different boundary conditions*, Journal of Mathematics Research, *14*(1) (2022), 30–45.

[6] H. Ali and M. Kamrujjaman, *Numerical solutions of nonlinear parabolic equations with Robin condition: Galerkin approach*, TWMS Journal of Applied and Engineering Mathematics, *12*(3) (2022), 851–863.

[7] I. Babuška, U. Banerjee, and J. E. Osborn, *Meshless generalized finite element methods: A survey of some major results*, Mesh free Methods for Partial Differential Equations, *26* (2003), 1–20.

[8] M. Bastoa, V. Semiao, and F. Calheiros, *Dynamics and synchronization of numerical solutions of the Burgers equation*, Journal of Computational and Applied Mathematics, *231* (2009), 793–806.

[9] A. BenRabah and O. A. Arqub, *An effective sustainable collocation method for solving regular/singular systems of conformable differential equations subject to initial constraint conditions*, Journal of Applied Analysis & Computation, *13*(3) (2023), 1336–1358.

[10] R. L. Burden and J. D. Faires, *Numerical analysis*, Brooks/Cole, USA, 2010.

[11] J. R. Cannon, Y. Lin, and A. L. Matheson, *The solution of the diffusion equation in two-space variables subject to the specification of mass*, Applied Analysis, *50*(1–2) (1993), 1–15.

[12] V. Capsso and K. Kunisch, *A reaction diffusion system arising in modeling man-environment diseases*, Quarterly of Applied Mathematics, *XLVI*, (3) (1988), 431–450.

[13] Z. Chen, *Finite element methods and their applications*, Springer Science and Business Media, 2005.

[14] A. Chen and C. Li, *An alternating direction galerkin method for a time-fractional partial differential equation with damping in two space dimensions*, Advances in Differential Equations, *356* (2017), 1–17.

[15] M. Dehghan, *Implicit locally one-dimensional methods for two-dimensional diffusion with a nonlocal boundary condition*, Mathematics and Computers in Simulation, *49*(4–5) (1999), 331–349.

[16] A. Ghoreyshi, M. Abbaszadeh, M. A. Zaky, and M. Dehghan, *An accurate and robust numerical method for solving distributed-order space–time fractional PDEs*, Zeitschrift für Angewandte Mathematik und Physik, *76*(242) (2025).

[17] A. Ghoreyshi, M. Abbaszadeh, M. A. Zaky, and M. Dehghan, *Finite block method for nonlinear time-fractional partial integro-differential equations: stability, convergence, and numerical analysis*, Applied Numerical Mathematics, *214* (2025), 82–103.

[18] A. Ghoreyshi, M. Abbaszadeh, M. A. Zaky, and M. Dehghan, *Two high-order numerical schemes based on the Lagrange polynomials for solving a distributed-order time-fractional partial integro-differential equation on non-rectangular domains*, Journal of Applied Mathematics and Computation, *71* (2025), 7271–7311.

[19] P. George, C. Maria, and G. Koutita, *A computational study with finite element method and finite difference method for 2D elliptic partial differential equations*, Applied Mathematics, *6*(12) (2015), 2104–2124.

[20] T. Grätsch and K. J. Bathe, *A posteriori error estimation techniques in practical finite element analysis*, Computers & Structures, *83*(4–5) (2005), 235–265.

[21] Y. Jiang and J. Ma, *High-order finite element methods for time-fractional partial differential equations*, Journal of Computational and Applied Mathematics, *235* (2011), 3285–3290.

[22] Y. W. Kwon and H. Bang, *The finite element method using MATLAB*, Mechanical and Aerospace Engineering Series, CRC Press, 2000.

[23] P. E. Lewis and J. P. Ward, *The finite element method (principles and applications)*, Addison-Wesley, 1991.

[24] S. A. Lima, M. Kamrujjaman, and M. S. Islam, *Direct approach to compute a class of reaction-diffusion equation by a finite element method*, Journal of Applied Mathematics and Computation, *4*(2) (2020), 26–33.

[25] S. A. Lima, M. Kamrujjaman, and M. S. Islam, *Numerical solution of convection-diffusion-reaction equations by a finite element method with error correlation*, AIP Advances, *11*(8) (2021), 085225(1–12).

[26] S. A. Lima, K. Mayeda and M. Kamrujjaman, *Advanced solutions of nonlinear convection-diffusion–reaction equations using the finite element method*, Nonlinear Science, *4* (2025), 100047.

[27] N. A. Mohamed, *Solving one and two-dimensional unsteady Burgers' equation using fully implicit finite difference schemes*, Arab Journal of Basic and Applied Sciences, *26* (2019), 254–268.

[28] S. Mohammad, *Smoothing of Crank-Nicolson schemes for the two-dimensional diffusion with an integral condition*, Applied Mathematics and Computation, *214* (2009), 512 – 522.

[29] M. Mohebujjaman, *High order efficient algorithm for computation of MHD flow ensembles*, arXiv preprint arXiv:2101.06852, 2021.

[30] M. Mohebujjaman, S. Shiraiwa, B. Labombard, J. C. Wright, and K. K. Uppalapati, *Scalability analysis of direct and iterative solvers used to model charging of superconducting pancake solenoids*, Engineering Research Express, *5*(1) (2023), 015045.

[31] M. Mohebujjaman, C. Buenrostro, M. Kamrujjaman, and T. Khan, *Decoupled algorithms for non-linearly coupled reaction–diffusion competition model with harvesting and stocking*, Journal of Computational and Applied Mathematics, *436* (2024), 115421.

[32] M. Moslem and R. *Sabry, Zakharov–Kuznetsov–Burgers equation for dust ion acoustic waves*, Chaos, Solitons & Fractals, *36*(3) (2008), 628-634.

[33] N. Mphephu, *Numerical solution of 1-D convection-diffusion-reaction equation*, MSc Thesis, University of Venda, African Institute for Mathematical Sciences, 2013.

[34] J. F. Neville, J. Xiao, and Y. Yan, *A finite element method for time fractional partial differential equations*, Fractional Calculus and Applied Analysis, *14*(3) (2011), 454–474.

[35] B. J. Noye, M. Dehghan , and J. van der Hoek, *Explicit finite difference methods for the two dimensional diffusion equation with a nonlocal boundary condition*, International Journal of Engineering Science, *32*(11) (1994), 1829-1834.

[36] S. S. Rao, *The finite element method in engineering*, Elsevier, 2010.

[37] M. M. Rashidi and E. Erfani, *New analytical method for solving Burgers' and nonlinear heat transfer equations and comparison with HAM*, Computer Physics Communications, *180*(9) (2009), 1539-1544.

[38] J. N. Reddy, *An introduction to nonlinear finite element analysis*, Oxford University Press, 2004.

[39] Y. Rucong, *A two–step shape–reserving advection scheme*, Advances in Atmospheric Sciences, *11* (1994), 479–490.

[40] G. D. Smith, *Numerical solution of partial differential equations: Finite difference methods*, Third Edition, Oxford University Press, New York, 1985.

[41] S. Wang, and Y. Lin , *A numerical method for the diffusion equation with nonlocal boundary specifications*, International Journal of Engineering Science, *28*(6) (1991), 543 – 546.

[42] Y. Wang, J. Jiang, and J. An, *Spectral- galerkin approximation based on reduced order scheme for fourth order equation and its eigenvalue problem with simply supported plate boundary conditions*, Journal of Applied Analysis & Computation, *14*(1) (2024), 61-83.

[43] A. M. Wazwaz, *Adomian decomposition method for a reliable treatment of the Bratu-type equations*, Applied Mathematics and Computation, *166* (2005), 652-663.